

# Development of the Human Pancreas From Foregut to Endocrine Commitment

Rachel E. Jennings,<sup>1,2</sup> Andrew A. Berry,<sup>1</sup> Rebecca Kirkwood-Wilson,<sup>1</sup> Neil A. Roberts,<sup>1</sup> Thomas Hearn,<sup>3</sup> Rachel J. Salisbury,<sup>1</sup> Jennifer Blaylock,<sup>1</sup> Karen Piper Hanley,<sup>1</sup> and Neil A. Hanley<sup>1,2</sup>

Knowledge of human pancreas development underpins our interpretation and exploitation of human pluripotent stem cell (PSC) differentiation toward a  $\beta$ -cell fate. However, almost no information exists on the early events of human pancreatic specification in the distal foregut, bud formation, and early development. Here, we have studied the expression profiles of key lineage-specific markers to understand differentiation and morphogenetic events during human pancreas development. The notochord was adjacent to the dorsal foregut endoderm during the fourth week of development before pancreatic duodenal homeobox-1 detection. In contrast to the published data from mouse embryos, during human pancreas development, we detected only a single-phase of Neurogenin 3 (NEUROG3) expression and endocrine differentiation from approximately 8 weeks, before which Nirenberg and Kim homeobox 2.2 (NKX2.2) was not observed in the pancreatic progenitor cell population. In addition to revealing a number of disparities in timing between human and mouse development, these data, directly assembled from human tissue, allow combinations of transcription factors to define sequential stages and differentiating pancreatic cell types. The data are anticipated to provide a useful reference point for stem cell researchers looking to differentiate human PSCs in vitro toward the pancreatic  $\beta$ -cell so as to model human development or enable drug discovery and potential cell therapy. *Diabetes* 62:3514–3522, 2013

The in vitro differentiation of embryonic stem cells (ESCs) or induced pluripotent stem cells (iPSCs) to pancreatic  $\beta$ -cells is an ambitious hope for cell therapy in diabetes, a tool for mechanistic understanding of monogenic diabetes, and a potential platform for drug discovery to promote  $\beta$ -cell regeneration (1,2). Most stem cell differentiation protocols aim to mimic normal development by steering pluripotent cells sequentially through endoderm, foregut, pancreatic progenitor, and then endocrine cell fates (1–4). Comprehensive knowledge of this pathway has come from extensive analyses of laboratory model species, such as mouse, chick, and frog (5–8). This has demonstrated

patterning of the foregut endoderm by transient proximity to the notochord that permits subsequent development of the dorsal pancreatic bud (9,10), with additional inductive influences provided by the dorsal aorta and other vasculature (11,12).

The intercellular signaling underlying these events and others has been mimicked as additives to the culture media during stem cell differentiation. In parallel, genetic inactivation in mouse has shown the sequential requirement for key transcription factors (5–8). Some of these factors, for which robust antibodies are available, have been used as phenotypic markers to indicate stages of  $\beta$ -cell differentiation from stem cells in vitro (2–4). Examples include SRY (sex determining region Y)-box-17 (SOX17), Gata-binding protein 4 (GATA4), forkhead box A2 (FOXA2), pancreatic and duodenal homeobox 1 (PDX1), two Nirenberg and Kim homeobox (NKX) factors, NKX6.1 and NKX2.2, and Neurogenin 3 (NEUROG3, also called NGN3) (5–8,13–15). Nevertheless, if the goal is to differentiate human stem cells by mimicking human development, this approach contains an assumption; namely, that human embryogenesis is very similar, if not identical, to that which occurs in small mammalian, avian, or amphibian species.

Research on human embryos is limited by availability and appropriate ethical restrictions. Previous data mostly arise from studies initiated at 7–8 weeks of fetal development, by which time the two pancreatic buds have coalesced as a single organ, and NEUROG3 detection implies endocrine commitment has already started (16–23). Subsequent profiles of transcription factors have been reported that culminate in the development of human islets from ~12 weeks of fetal age (18,21,23). In stark contrast, knowledge of earlier events is exceptionally restricted; for instance, the detection of PDX1 in a single dorsal pancreatic bud at ~4 weeks of development and SOX9 transcripts by mRNA in situ hybridization soon after (20,24). Foregut development, the potential for patterning by nearby structures, and gene expression profiles during pancreatic bud formation, pancreatic growth, and early lineage differentiation has remained unexplored despite being essential for  $\beta$ -cell development. Here, we describe these early developmental events in a series of human embryos. The data help to minimize current interspecies assumptions made about stem cell differentiation, identify simple transcription factor combinations that signify differentiating pancreatic cell types, and provide a reference point for the validity of using stem cells at a particular stage of differentiation to model human developmental mechanisms in vitro.

## RESEARCH DESIGN AND METHODS

**Human tissue collection.** The collection, use, and storage of human embryonic and fetal tissue ( $n = 31$ ) was done with ethical approval from the North West Research Ethics Committee, under the codes of practice issued by the

From the <sup>1</sup>Centre for Endocrinology and Diabetes, Institute of Human Development, Faculty of Medical & Human Sciences, Manchester Academic Health Sciences Centre, University of Manchester, Manchester, U.K.; the <sup>2</sup>Endocrinology Department, Central Manchester University Hospitals National Health Service Foundation Trust, Manchester, U.K.; and the <sup>3</sup>Centre for Human Development, Stem Cells and Regeneration, Human Genetics, University of Southampton, Southampton General Hospital, Southampton, U.K.

Corresponding author: Neil A. Hanley, neil.hanley@manchester.ac.uk.

Received 25 October 2012 and accepted 20 April 2013.

DOI: 10.2337/db12-1479

This article contains Supplementary Data online at <http://diabetes.diabetesjournals.org/lookup/suppl/doi:10.2337/db12-1479/-/DC1>.

© 2013 by the American Diabetes Association. Readers may use this article as long as the work is properly cited, the use is educational and not for profit, and the work is not altered. See <http://creativecommons.org/licenses/by-nc-nd/3.0/> for details.

Human Tissue Authority and legislation of the U.K. Human Tissue Act 2008. Details on collection and handling are as described previously (20). In brief, human embryos and fetuses were collected from medical and surgical terminations of pregnancy. Specimens for immunohistochemistry were fixed within 1 h in 4% paraformaldehyde before processing and embedding in paraffin wax. Sectioning took place at 5- $\mu$ m intervals, with every eighth section taken for hematoxylin and eosin staining to confirm morphology and anatomical landmarks.

**Immunohistochemistry and cell counting.** Immunohistochemistry was performed as described previously (20) using the primary antibodies listed in Supplementary Table 1 in at least three specimens per stage. For cell counting, cells that were positively stained for nuclear NGN3 or insulin were quantified per total number of pancreatic epithelial cells in at least three tissue sections from at least two embryos or fetuses. The study was restricted to immunohistochemistry using effective commercial antibodies readily available to stem cell researchers. In our hands, this precluded current robust examination of pancreas-specific transcription factor 1A (PTF1A), hepatocyte nuclear factor 1 $\beta$  (HNF1 $\beta$ ), hematopoietically expressed homeobox (HHEX), motor neuron and pancreas homeobox 1 (MXN1), GATA6, and ONECUT6, all of which are important for pancreas development (5–8,25–27).

**Isolation of RNA, reverse transcription, and real-time quantitative PCR.** Total RNA was isolated, cDNA generated, and quantitative PCR performed as in previous studies from at least three specimens at each stage of late embryonic and early fetal pancreas (47 days postconception [dpc]–10 weeks postconception [wpc]) (17). RNA purity and quantity was assessed using a NanoDrop spectrophotometer (NanoDrop Technologies, Rockland, DE) to measure the 260-to-280 and 260-to-230 ratios of absorbance (nm).

## RESULTS

Postimplantation human embryos are classified by Carnegie stage (CS), which uses morphology visible by light microscopy to ascribe stages that can be correlated to embryonic days (e) of mouse development (Supplementary Table 2). At CS9, which occurs at 22–26 dpc and is defined by the presence of up to 4 somite pairs, the definitive endoderm openly communicated along much of the embryo's anterior-posterior axis with the visceral endoderm of the yolk sac (Fig. 1A, long double-headed arrow). However, by CS10 (25–27 dpc; 4–12 somites), folding in the head and "tail" regions and along both flanks had created the blind-ending tubes of foregut and hindgut, thereby restricting the opening of the yolk sac to the intervening midgut (Fig. 1A, short double-headed arrow). The anterior end of this opening constitutes the foregut-midgut boundary and is termed the anterior intestinal portal (AIP). It allows demarcation of the most distal region of foregut from where the dorsal and ventral pancreatic buds (and liver) arise. In three CS10 embryos, the dorsal foregut epithelium at this location was a single cell thick and adjacent to the notochord (Fig. 1B and C). In chick embryos, the immediacy of the notochord causes exclusion of sonic hedgehog (Shh) expression from the dorsal foregut endoderm, which, in turn, allows later expression of *Pdx1* and dorsal pancreatic budding (10). A similar exclusion of SHH was visible in human embryos at CS10 (Fig. 1D, arrow), extending across the entire dorsal surface of the endoderm, in contrast to the detection of SHH throughout the thicker pseudostriated epithelium of the ventrolateral endoderm adjacent to the lateral mesoderm (Fig. 1D, arrowhead). This pattern of SHH detection was observed from the level of the second to the ninth somites. Nuclear FOXA2 was present in all of the epithelial cells of the endoderm (Fig. 1E), whereas SOX17 was restricted to the region that lacked SHH (Fig. 1F, arrowhead). At this stage of development, neither GATA4 nor PDX1 were detected in the foregut (Fig. 1G and data not shown).

The proximity between notochord and gut is possible until the paired dorsal aortae intervene and fuse in the midline with its surrounding mesoderm, which had occurred by

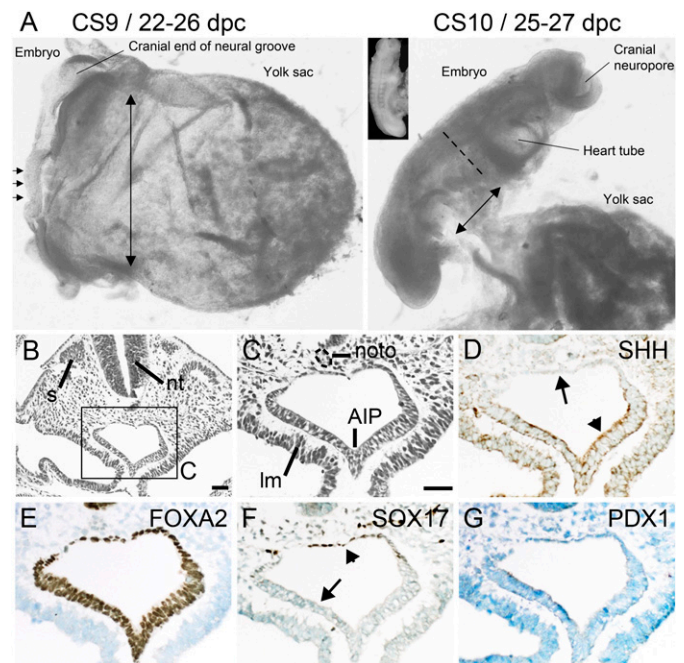


**FIG. 1. Early foregut endoderm and its proximity to the notochord.** A: Human embryos at CS9/22–26 dpc (the small horizontal arrows indicate three somite pairs) and CS10/25–27 dpc (11 somite pairs, visible in the inset). At CS9, the double-ended arrow highlights the large communication between the gut tube/definitive endoderm and the yolk sac compared with its restriction at CS10 (smaller double-ended arrow). The dashed line indicates the level of the AIP at CS10. Bright-field transverse images at CS 10/25–27 dpc stained with hematoxylin and eosin (B and C) or toluidine blue after immunohistochemistry (brown) for SHH, FOXA2, SOX17, and PDX1 (D–G). Arrows and arrowheads point to absence of and detection of SHH (D) and SOX17 (F), respectively. lm, lateral mesoderm; noto, notochord; nt, neural tube; s, somite. The CS9 embryo is 2 mm in length; scale bars represent 50  $\mu$ m (B and C–G).

CS12 (29–31 dpc). At this stage, PDX1 was first apparent over stretches of  $\sim$ 15 cells immediately anterior to the AIP (Fig. 2A–C). In keeping with the thicker ventral wall of the foregut at CS10, the ventral domain of PDX1 contained approximately twice as many cells as its dorsal counterpart. The presumptive duodenal-pancreatic endoderm also contained nuclear GATA4, FOXA2, and SOX17 (Fig. 2D–F). Expression of these three transcription factors extended posterior to the AIP into the distal duodenum/midgut. In contrast, SOX9 was predominantly expressed in the hepatic bud with FOXA2 and was only very weakly colocalized with PDX1 (Fig. 2C, E, G, and I). NKX6.1 and NKX2.2 were not detected in the endoderm at this stage but were detected in the neural tube (Fig. 2H and data not shown).

At CS13 (30–33 dpc), distinct buds of dorsal and ventral pancreas were visible, the latter lying just posterior to the embryonic gall bladder (Fig. 3A and B). Both pancreatic buds were within a few cells from the ventral and dorsal anastomoses of the left and right vitelline veins, which eventually form the portal vein, and contained microlumens (Fig. 3D, inset). Ventral and dorsal pancreatic cells and the intervening duodenum were uniformly positive for nuclear PDX1, with weaker staining extending into the extrahepatic biliary duct and the gall bladder (Fig. 3C). GATA4 was also apparent within pancreatic and duodenal cells and was extended into the gall bladder but was barely detected in the extrahepatic biliary duct (Fig. 3D). It was also present in the mesenchymal cells surrounding the hepatic cords and gallbladder. SOX9 was extensively

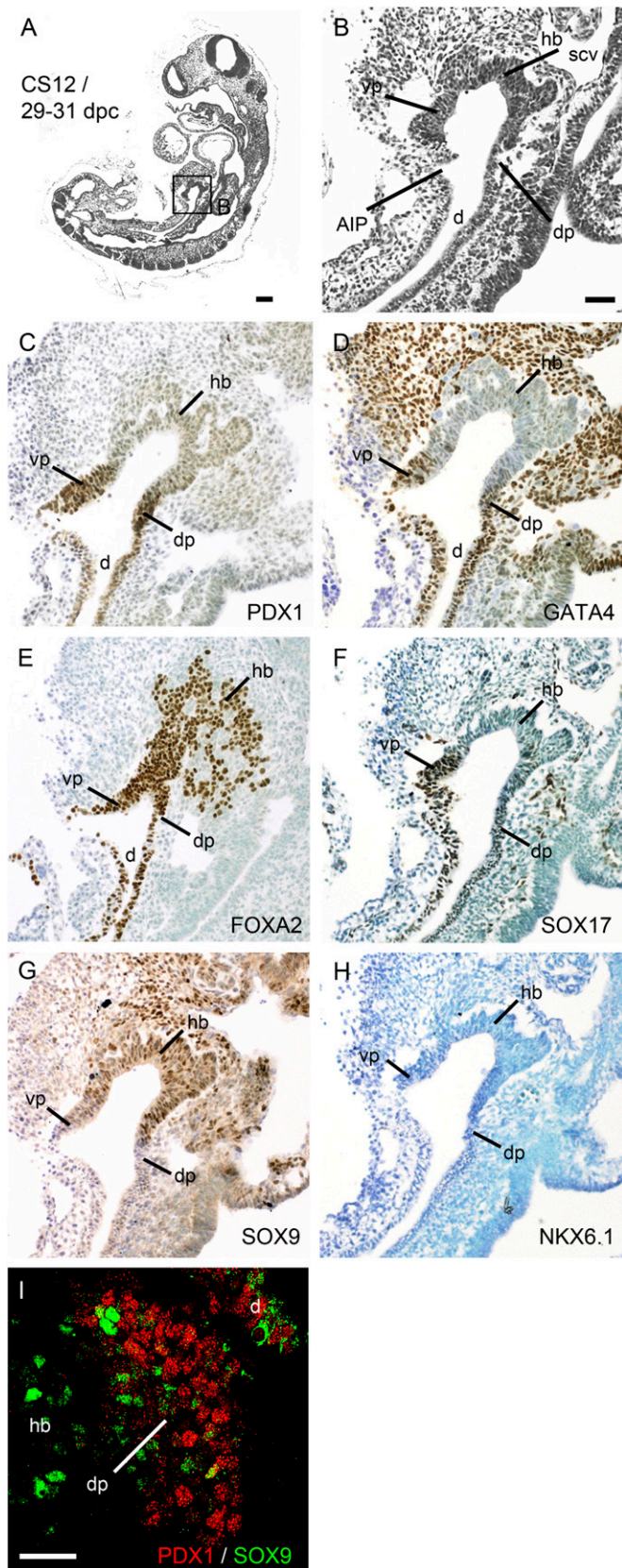


**FIG. 2.** Pancreatic endoderm in the distal foregut. Sagittal sections of a human embryo at CS 12/29–31 dpc stained with hematoxylin and eosin (A and B) or toluidine blue after immunohistochemistry (brown) for PDX1 (C), GATA4 (D), FOXA2 (E), SOX17 (F), SOX9 (G), and NKX6.1 (H). The boxed area in A is shown at higher magnification in B. I: Dual immunofluorescence at CS12 showing minimal PDX1 (red) and

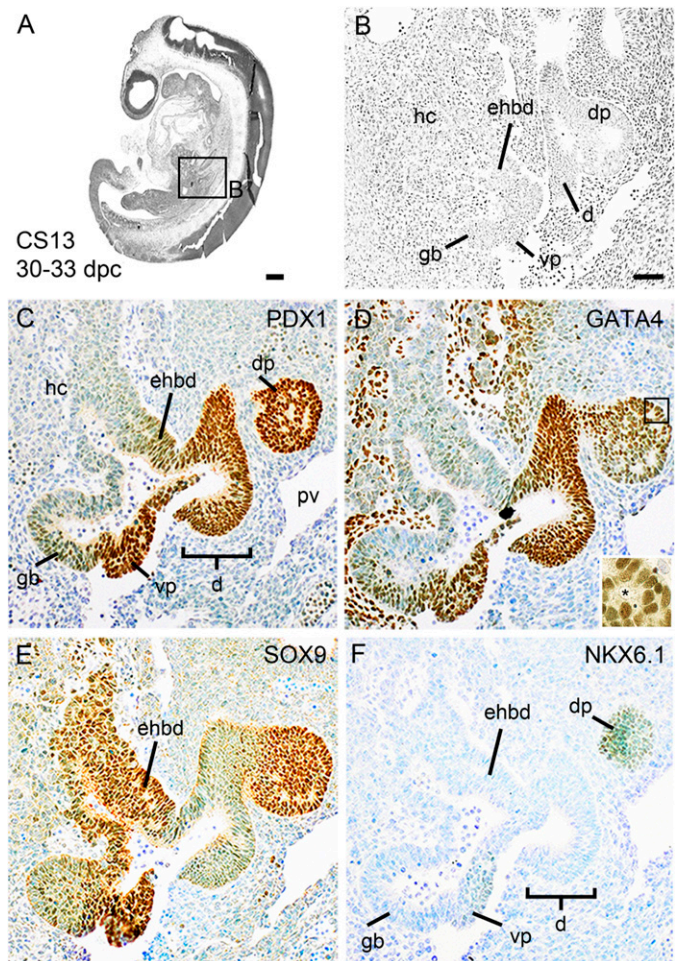


**FIG. 3.** Pancreatic bud formation. Sagittal sections of a human embryo at CS 13/30–33 dpc stained with hematoxylin and eosin (A and B) or toluidine blue after immunohistochemistry (brown) for PDX1 (C), GATA4 (D), SOX9 (E), and NKX6.1 (F). The boxed area in A is shown at higher magnification in B. The inset in D demonstrates microlumen formation. dp, dorsal pancreatic bud; vp, ventral pancreatic bud; hc, hepatic cords; gb, gallbladder; d, duodenum; ehbd, extrahepatic bile duct; pv, portal vein. Scale bars represent 200  $\mu$ m (A) and 100  $\mu$ m (B–F).

detected in the dorsal and ventral pancreas as well as in the extrahepatic biliary duct but was only weakly detected in the duodenum and gall bladder (Fig. 3E). At this stage, pancreatic NKX6.1 was first detected, most readily in the dorsal bud, but NKX2.2 remained absent (Fig. 3F and data not shown). In line with earlier (and later stages), FOXA2 uniformly stained all epithelial cell nuclei in the branching hepatic cords, extrahepatic biliary duct, duodenum, and pancreas; in contrast, SOX17 was no longer detected at this or later stages within the duodenum or pancreas but was present in the embryonic gallbladder (data not shown).

By CS15 (35–37 dpc), the pancreas was widely separated from the aorta; however, gut rotation had brought both ventral and dorsal pancreatic buds to either side of the portal vein (Fig. 4A–C). The epithelial cells contained nuclei that stained uniformly for PDX1, FOXA2, SOX9, and

SOX9 (green) colocalization. d, duodenum; dp, dorsal pancreatic endoderm; hb, hepatic bud; scv, right subcardinal vein; vp, ventral pancreatic endoderm. Scale bars represent 200  $\mu$ m (A), 100  $\mu$ m (B–H), and 50  $\mu$ m (I).

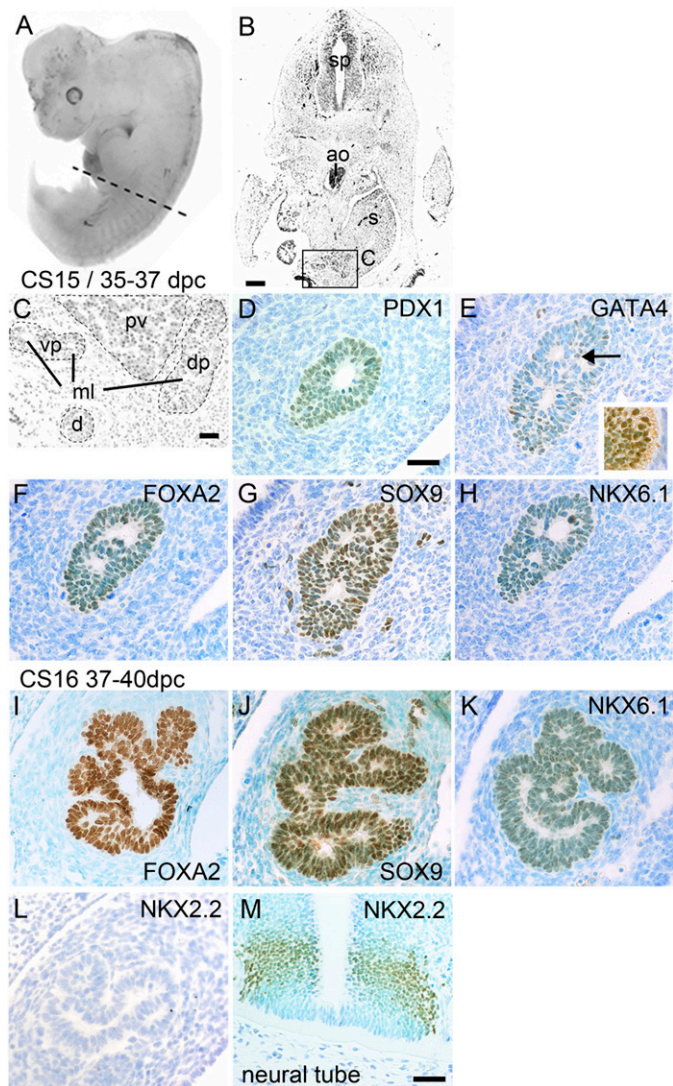


**FIG. 4.** Development of a branched embryonic pancreas. **A:** Human embryo at CS15/35–37 dpc. The broken line in **A** shows the level of the transverse section in **B**. **B:** Transverse section stained with hematoxylin and eosin; the boxed area containing the pancreas is shown at higher magnification in **C**. Note the separation of aorta from the pancreas. Sections stained with toluidine blue after immunohistochemistry (brown) for PDX1 (**D**), GATA4 (**E**, arrow shows positive nucleus), FOXA2 (**F**), SOX9 (**G**), and NKX6.1 (**H**). The inset in **E** demonstrates positive GATA4 staining in stomach epithelium. Sections of a human embryo at CS16/37–40 dpc stained with toluidine blue after immunohistochemistry (brown) for FOXA2 (**I**), SOX9 (**J**), NKX6.1 (**K**), and NKX2.2 (**L** and **M**). Note the lack of detection of NKX2.2 in pancreas (**L**) compared with ventral neural tube (**M**). ao, aorta; d, duodenum; dp/vp, dorsal/ventral pancreas; ml, micro-lumen; pv, portal vein; s, stomach; sp, spinal cord. Scale bars represent 200  $\mu\text{m}$  (**B**), 50  $\mu\text{m}$  (**C** and **D–L**), and 25  $\mu\text{m}$  (**M**).

NKX6.1 (Fig. 4D, F–H). GATA4 was present in the stomach epithelium (Fig. 4E, inset) but was barely detected in the pancreas compared with levels found at CS13, except for some occasional stained nuclei scattered throughout the pancreas (Fig. 4E, arrow). These transcription factor profiles were the same at CS16 (37–40 dpc; Fig. 4I–K and data not shown), by which time the epithelium was mostly one or two cells thick and clearly branched, with peripheral and more centrally located cells (Fig. 4I–K). As in earlier stages, NKX2.2 was not detected in the pancreas (Fig. 4L) but was present in the ventral neural tube (Fig. 4M). The lack of pancreatic NKX2.2 corresponded to negligible

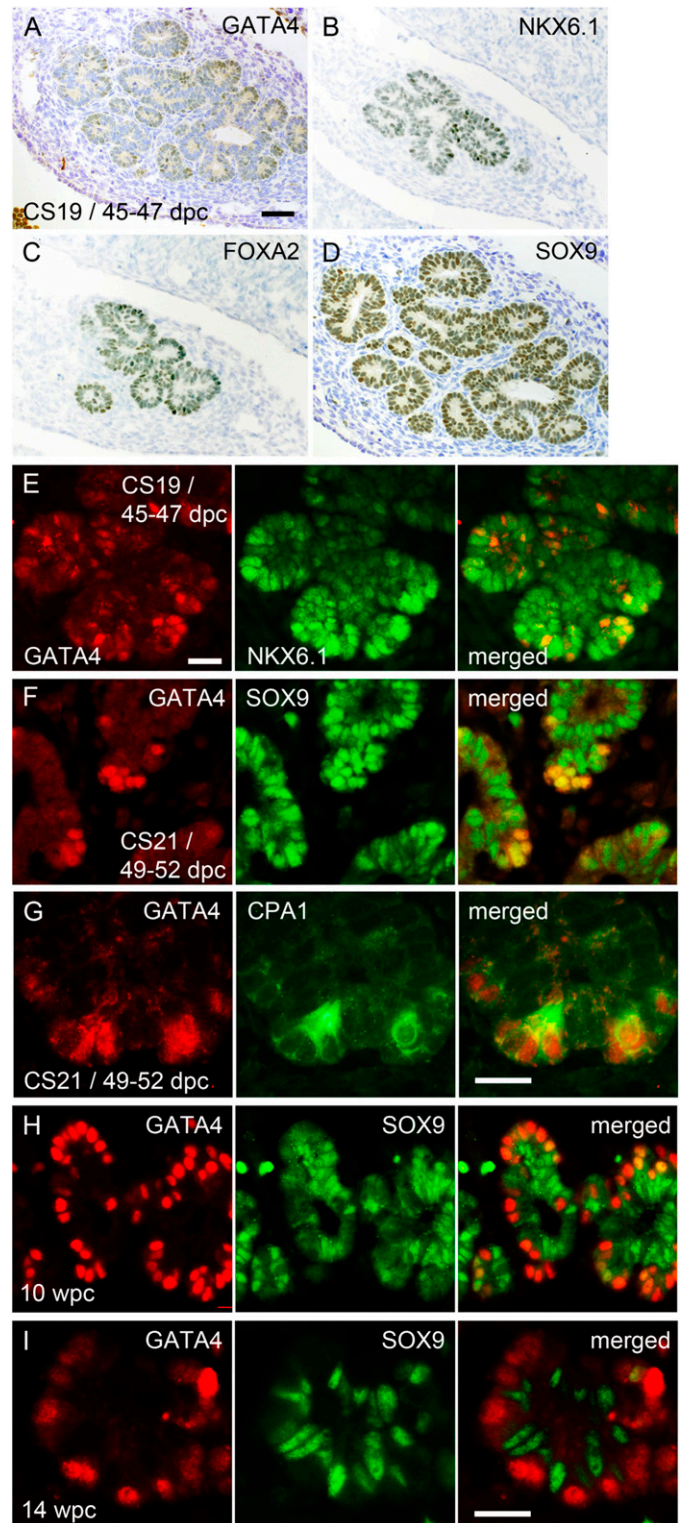


**FIG. 5.** Differentiation of the exocrine lineage. Sections through the pancreas of a human embryo at CS19/45–47 dpc stained with toluidine blue after immunohistochemistry (brown) for GATA4 (**A**), NKX6.1 (**B**), FOXA2 (**C**), and SOX9 (**D**) or immunofluorescence for GATA4 (red) and NKX6.1 (green) (**E**). Sections through the pancreas at CS21/49–52 dpc (**F** and **G**), 10 wpc (**H**), and 14 wpc (**I**). Immunofluorescence is shown for GATA4 (red) and SOX9 or CPA1 (green). Scale bars represent 50  $\mu\text{m}$  (**A–D**), 25  $\mu\text{m}$  (**E–H**).

pancreatic reads (<1 read per kilobase per million base pairs) for NKX2.2 transcripts in unpublished RNA-seq datasets at CS13–15).

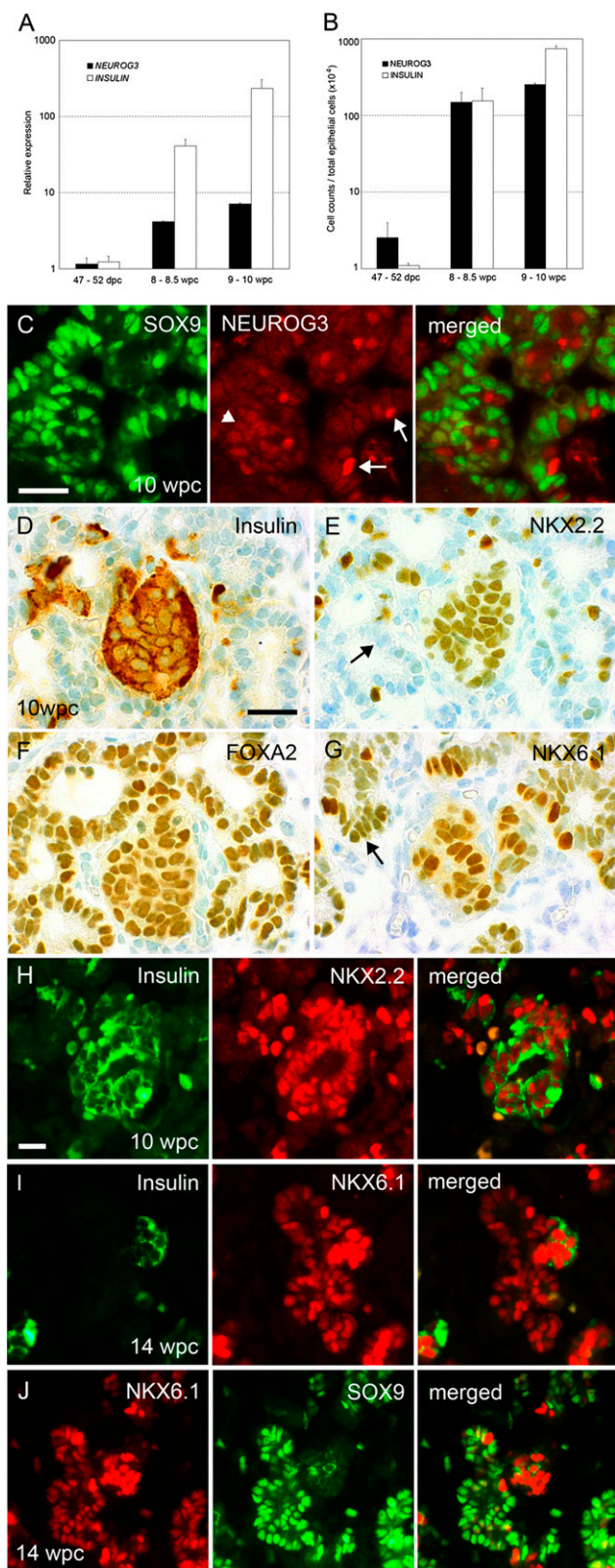


**FIG. 6.** Early differentiation of the endocrine lineage. Quantification of the onset of *NEUROG3* and *INSULIN* expression by quantitative PCR (**A**) and cell count per total pancreatic epithelial cell number (**B**) in human pancreas from 47–52 dpc to 9–10 wpc. Bars show mean  $\pm$  SE from at least two specimens. **C**: Sections through the pancreas at 10 wpc after immunofluorescence for *SOX9* (green) and *NEUROG3* (red). Arrows point to nuclei robustly stained for *NEUROG3* and negative for *SOX9*; arrowheads show weak anti-*NEUROG3* immunoreactivity in *SOX9*-positive cells. Serial sections through the pancreas at 10 wpc

During mouse development, commitment of the acinar cell lineage from the pool of multipotent progenitor cells is largely complete by  $\sim$  e14 (13,28–30). These cells, located at the tips of a branched pancreas, contain *Gata4* but lack *Nkx6.1* and *Sox9* compared with the trunk cells that express *Nkx6.1* and *Sox9* but lack *Gata4* (13,29–32). During human development at CS19 (45–47 dpc) *GATA4* was clearly apparent for the first time in the nuclei of some peripheral cells but was restricted from the central trunks (Fig. 5A). Cells in both locations still contained nuclear *NKX6.1*, *FOXA2*, and *SOX9* at CS19 and CS21 (49–52 dpc), when the peripheral *GATA4*-positive tip cells also immunostained for carboxypeptidase A1 (CPA1; Fig. 5B–G, and data not shown). By 10 wpc ( $\sim$ 2.5 weeks later), the CPA1/*GATA4*-positive tip cells uniformly lacked *NKX6.1* (data not shown) and mostly lacked *SOX9* (Fig. 5H). By 14 wpc, *GATA4* and *SOX9* detection was almost entirely mutually exclusive, implying terminal differentiation of *GATA4*-containing acinar cells surrounding *SOX9*-positive centroacinar (and ductal) cells (Fig. 5J).

In mouse, cells in the trunk domain are characterized by *Nkx6.1*, *Sox9*, and *Hnf1 $\beta$*  expression and possess the potential for duct or, if they transiently produce *Neurog3*, endocrine differentiation (5–8,13,29,33). Murine *Neurog3* expression is biphasic, with an initial wave from e8.5 to e11 (34). The second phase starts at e12, peaks at e15.5, and is much reduced by e18.5. We did not detect *NEUROG3*, insulin, or glucagon as protein or transcripts to correlate with the first phase of expression in mouse (Supplementary Fig. 1). The increase in *NEUROG3* expression and of *NEUROG3*-positive cells during late embryogenesis was closely timed to the appearance of fetal insulin (Fig. 6A and B). Compared with CS20–21 (47–52 dpc), *NEUROG3* transcripts had increased 3.6-fold by 8–8.5 wpc and 6.1-fold by 9–10 wpc, with corresponding increases in *INSULIN* of 34-fold and 193-fold. Cell counting at the same time points produced increases of 59- and 102-fold for *NEUROG3*-positive cells and 140- and 684-fold for insulin-positive cells. Nuclear *SOX9* was absent in all cells with robust *NEUROG3* detection (Fig. 6C) and in insulin-positive cells (data not shown); however, by increasing the imaging gain and using more concentrated primary antibody, a weak anti-*NEUROG3* signal could be gained in some *SOX9*-positive cells. Clusters of fetal  $\beta$ -cells were apparent at 10 wpc (Fig. 6D), which contained *NKX2.2*, *FOXA2*, and *NKX6.1* in serial sections (Fig. 6E–G); however, as in earlier embryogenesis, *NKX2.2* was absent from the trunk progenitor domain (Fig. 6E, arrow) that contained *FOXA2*, *NKX6.1* (Fig. 6F and G, arrow), and *SOX9* (Fig. 6C). These data were confirmed by immunofluorescence, which showed *NKX2.2* was largely restricted to  $\beta$ -cells at 10 wpc (Fig. 6H), whereas *NKX6.1* still colocalized extensively with *SOX9* in duct-like cells as well as with insulin in  $\beta$ -cells at 14 wpc (Fig. 6I and J).

## DISCUSSION

By the time pregnancy can be confirmed biochemically (i.e., once menstruation has been clearly postponed), the

stained with toluidine blue after immunohistochemistry (brown) for insulin (**D**), *NKX2.2* (**E**), *FOXA2* (**F**), and *NKX6.1* (**G**). Arrows in **E** and **G** point to duct-like epithelium negative for *NKX2.2* but stained for *NKX6.1*. Sections through the pancreas at 10 wpc (**H**) and 14 wpc (**I** and **J**) after dual immunofluorescence for insulin (green) with *NKX2.2* or *NKX6.1* (red) (**H** and **I**), and *NKX6.1* (red) with *SOX9* (green) (**J**). Scale bars represent 25  $\mu$ m (**C–J**).

embryo has most commonly developed for 3 weeks or longer. Under ethically approved programs of accessing human material from social or voluntary termination of pregnancy, it is thus impossible to research gastrulation and very early lineage commitment (35). Thereafter, potential comparison can be made with early events in model species, although such reports in human tissue are rare. This study aimed to describe human pancreas development up to and including endocrine commitment, after which other reports have detailed the appearance of NEUROG3 and subsequent islet development (16–23). The purpose was to complement data acquired in mouse and chick models (5–8) and to provide defining features of the early human pancreas to match the growing need for assessment of human stem cells differentiated to different points along the pathway to a pancreatic  $\beta$ -cell fate (2,4) (Table 1 and Fig. 7).

After gastrulation, the earliest patterning event leading to pancreas development is the exclusion of SHH from the dorsal endoderm where it contacts the notochord. This was originally described in chick and is mediated in part by activin signaling from the notochord (10). In human embryos, just before 3 weeks of development (CS10), the extent of SHH exclusion was consistent with fate mapping in chick, which demonstrated that the dorsal pancreas is made up of endoderm cells that originated from between the third and ninth somites (6). Additional patterning of pancreatic endoderm comes from vessels. In mouse and chick, the dorsal aorta induces pancreas development and,

specifically, promotes insulin expression in the dorsal pancreatic endoderm (11). This occurs before separation of the pancreatic endoderm from the two aortae by the intervening splanchnic mesoderm (36). At the level of the AIP, the paired dorsal aorta did not contact the dorsal endoderm, perhaps explaining why an early phase of endocrine differentiation was not apparent at this site in human embryos by insulin, glucagon, or NEUROG3 detection. GATA4 was not apparent in the foregut at CS10 (when it was robustly detected in developing human heart; data not shown), which was surprising when it is one of the key factors for gut closure in mouse (37,38). In mouse, Sox17 has been variably reported as absent from the foregut at e8.5 (39) or colocalized with Pdx1 in ventral endoderm, before becoming restricted to the primordial gall bladder by e10.5 (40). This latter study corresponds to our data in human embryos at CS12 (29–31 dpc) and in the embryonic gallbladder at CS13 (30–33 dpc). However, before this, SOX17 was also detected in the SHH-negative cells of dorsal foregut at CS10 (which corresponds to e8–8.5; Supplementary Table 2) at the level of the AIP (Fig. 1F) and more cranially (Supplementary Fig. 2).

Acquiring multipotent pancreatic progenitors is a key step in the differentiation of human ESCs/IPSCs toward the pancreatic  $\beta$ -cell (1,2,4). From studies mostly in mouse, several transcription factors are critical for establishment and proliferation of multipotent pancreatic progenitors, including Pdx1, Ptf1a, Sox9, Mnx1, and Foxa2 (5–8,41). In human embryos, robust PDX1 detection was

TABLE 1  
Comparison of pancreas development between mouse and human

Event during mouse development	Event during human development
Foregut development, pancreatic specification, and bud formation	
Pdx1 in dorsal endoderm (i.e., pancreatic specification) while adjacent to the notochord and dorsal aortae (by e8.75/10 somite pairs, before gut closure) (5–8,42)	PDX1 not detected at late CS10/11 somite pairs; first apparent at CS12 (21–29 somite pairs) after gut closure once mesenchyme has separated notochord and aorta from dorsal foregut
Gata4 present in ventral foregut endoderm at e8; important for gut closure (37,38,43)	GATA4 not detected in foregut endoderm at CS10; detected later at CS12
Sox17 not detected in dorsal foregut endoderm at e8.5, variably detected in ventral foregut endoderm (39,40)	SOX17 detected in dorsal foregut endoderm at CS10 and CS12; detected in ventral endoderm at CS12
Multipotent pancreatic progenitors	
Nkx2.2 marks multipotent pancreatic progenitors before endocrine commitment (6,14,15)	NKX2.2 not detected in pancreatic progenitors before endocrine commitment
Differentiation of the acinar lineage	
Nkx6.1 excluded from tip cells by e14.5 (CS19–20) (13)	NKX6.1 still detected in peripheral cells at CS21
Gata4 localized to tip cells with Sox9 exclusion by e16.5 (CS23) (31–33)	GATA4 in peripheral cells and excluded from trunk cells at CS19; GATA4 colocalization with CPA1 at CS21; however, SOX9 exclusion in acinar cells only completed between 10–14 wpc
Differentiation of the endocrine lineage	
Two phases of Neurog3 during embryogenesis; the second major phase (so-called secondary transition) occurs from ~e12 (CS15) until e18, peaking at ~e15.5 (CS21–22) (34)	One phase of NEUROG3, which only starts near the end of embryogenesis (CS21–22), followed by $\beta$ -cell differentiation
Islets only formed close to birth (e19–21) (5–8)	Islets apparent at 12 wpc (20)

In the left column, timings in italics are the anticipated human equivalent of the mouse developmental stage; the actual timing of the event during human development is provided in the right column.

initially accompanied by only very weak detection of SOX9 in presumptive pancreatic endoderm, which by CS12 (29–31 dpc) also expressed GATA4, SOX17, and FOXA2. Recent data in mouse have shown that Gata factors are required at least in part for appropriate Pdx1 expression (25) if not its initiation (26). After this, SOX17 was lost from the pancreatic buds, SOX9 was strongly detected, and NKX6.1 was first apparent. From our examinations over the next 2 weeks, this profile of PDX1, SOX9, NKX6.1, and FOXA2 would distinguish multipotent pancreatic progenitors in human ESC/IPSC differentiation protocols (without NKX6.1, a combination of FOXA2, SOX9, and weak PDX1 detection could indicate extrahepatic biliary duct cells) (Fig. 7). Previously, NKX6.1 has only been reported in human pancreas with the onset of  $\beta$ -cell differentiation (18). An unexpected difference from studies in mouse was the absence of pancreatic NKX2.2 in human embryos before endocrine differentiation. Although *Nkx2.2* is present in multipotent progenitors in mouse (14), our data are consistent with it being dispensable for pancreatic progenitor development but essential for  $\beta$ -cell formation (14,15) (Table 1). Endocrine commitment, by virtue of nuclear NEUROG3 detection in central pancreatic epithelial cells, commenced at the end of the embryonic period tightly correlated to the appearance of fetal  $\beta$ -cells containing insulin. From our

data here and previous observations (17,18,20,23), the detection of NEUROG3 in differentiating human ESCs/IPSCs should correlate with the loss of SOX9 and the subsequent detection of nuclear NKX2.2, NKX6.1, PDX1, and ISL1.

Our data demonstrate that the phases of pancreas development are the same between mouse and human, with the demarcation of pancreatic domains in the ventral and dorsal foregut, bud formation, and outgrowth, followed by differentiation of the separate pancreatic lineages (5–8). However, differences in timing are apparent between the two species. This is not simply a reflection of longer human gestation, because embryogenesis can be compared directly across species (Supplementary Table 2). In human embryos, PDX1 was only detected after the endoderm was separated from the notochord and aorta(e) by mesenchyme. In mouse, it occurs earlier (e8.5–8.75, 10 somite pairs) while the dorsal foregut still contacts these structures (42) (the CS10 human embryo in Fig. 1, which lacked PDX1, already contained 11 somite pairs). Transcription factor profiles were also slow to resolve during acinar differentiation. In mouse, Gata4-positive acinar cells arise from multipotent precursors that expressed Pdx1, Hnf1b, Ptf1a, Sox9, and Nkx6.1 (5–8,41). The commitment of these cells with the exclusion of Nkx6.1 and Sox9 is largely complete by e14–e14.5 (13,28,29,33), which corresponds to

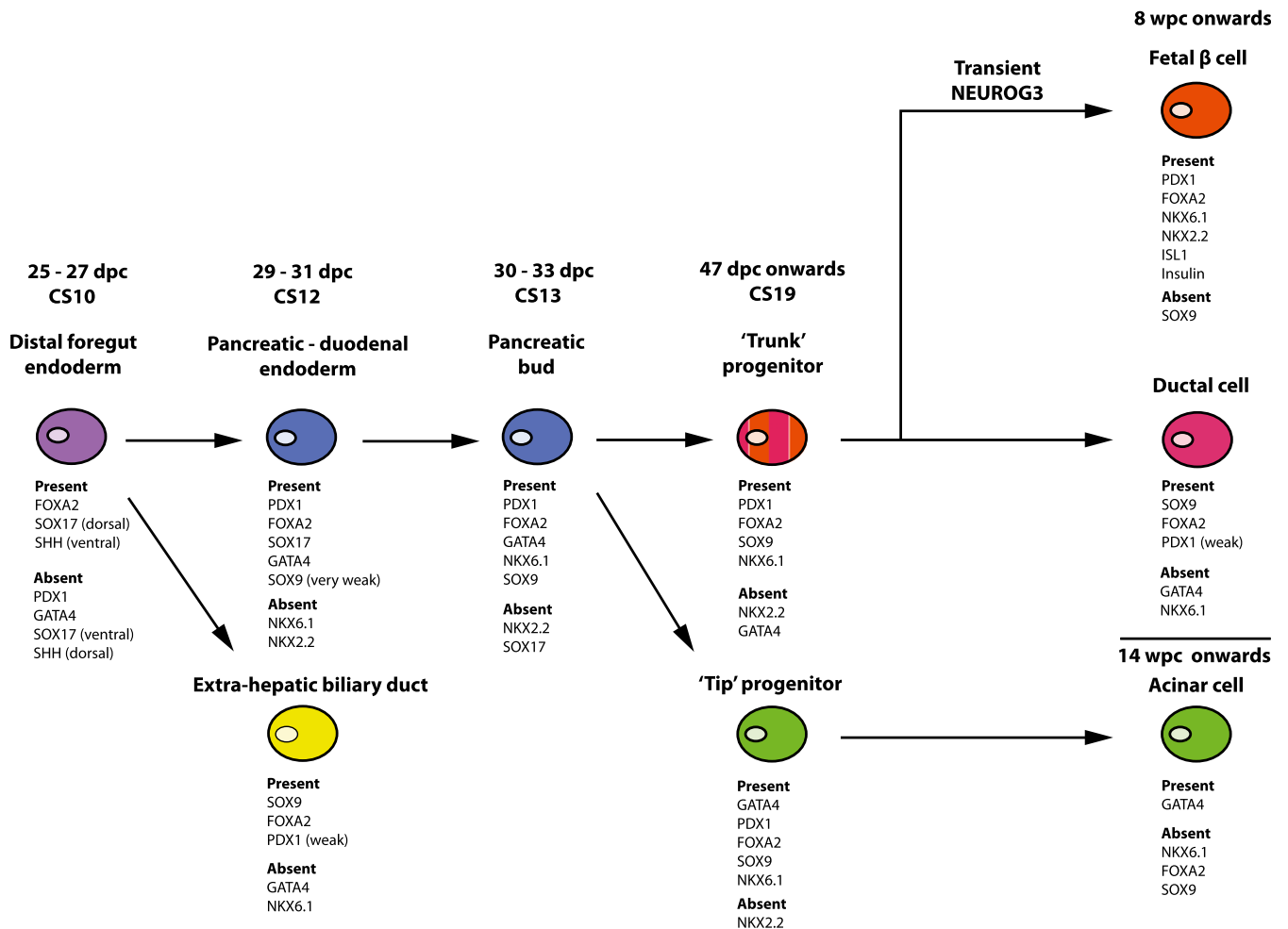


**FIG. 7. Transcription factors to define different cell types and stages of differentiation for the early human pancreas.** Combinations of transcription factors (plus SHH and insulin) are shown to identify different cell types and stages of development for the foregut, extrahepatic biliary duct, and pancreas based on the current data and previous immunohistochemical studies by us and others (18,20,23).

approximately CS19 (45–47 dpc). In human pancreas, however, these peripheral GATA4-positive cells uniformly possessed NKX6.1 and SOX9 at CS19 and for at least another week of development (CS21 [49–52 dpc], when they also contained CPA1). GATA4 expression still overlapped partially with SOX9 expression at 10 wpc. It was only by 14 wpc that expression profiles for GATA4 and SOX9 had fully resolved to acinar and centroacinar populations, respectively. Thus, differentiating human ESCs/IPSCs, which according to mouse development seemingly possess a mixed profile of transcription factors, might actually still represent normal human development rather than an aberrant cell type.

In summary, our data do not support an early phase of endocrine differentiation in human embryos analogous to primary transition during mouse development, and we did not observe NKX2.2 in the pancreatic progenitor population before endocrine commitment. Instead, the current data provide combinations of transcription factors directly in human tissue that can describe the different cell types and stages of early human pancreas development (Fig. 7). We anticipate that this combinatorial approach using commercial reagents will assist in the characterization of cells differentiated in vitro from human ESCs/IPSCs toward pancreatic  $\beta$ -cells.

#### ACKNOWLEDGMENTS

R.E.J. is a Medical Research Council (MRC) clinical training fellow. N.A.H. is a Wellcome Trust senior fellow in clinical science (WT088566MA). R.J.S. is an MRC doctoral account PhD student. N.A.R. held a Kerkut Trust PhD studentship awarded to K.P.H. This work was also supported by an Innovation Grant from the Juvenile Diabetes Research Foundation, the Manchester Biomedical Research Centre, and a Wellcome Trust Institutional Strategic Support Fund (WT097820MF).

No potential conflicts of interest relevant to this article were reported.

R.E.J., A.A.B., R.K.-W., N.A.R., T.H., R.J.S., J.B., and N.A.H. researched data. R.E.J. and N.A.H. co-wrote the manuscript. K.P.H. reviewed and edited the manuscript and contributed to discussion. N.A.H. oversaw the collection of human material. N.A.H. is the guarantor of this work and, as such, had full access to all the data in the study and takes responsibility for the integrity of the data and the accuracy of the data analysis.

The authors are grateful for the assistance of research nurses, Cellins Vinod and Leena Abi, and clinical colleagues at St. Mary's Hospital and Central Manchester University Hospitals National Health Service Foundation Trust.

#### REFERENCES

- Best M, Carroll M, Hanley NA, Piper Hanley K. Embryonic stem cells to beta-cells by understanding pancreas development. *Mol Cell Endocrinol* 2008;288:86–94
- Docherty K, Bernardo AS, Vallier L. Embryonic stem cell therapy for diabetes mellitus. *Semin Cell Dev Biol* 2007;18:827–838
- D'Amour KA, Agulnick AD, Eliazar S, Kelly OG, Kroon E, Baetge EE. Efficient differentiation of human embryonic stem cells to definitive endoderm. *Nat Biotechnol* 2005;23:1534–1541
- Kroon E, Martinson LA, Kadoya K, et al. Pancreatic endoderm derived from human embryonic stem cells generates glucose-responsive insulin-secreting cells in vivo. *Nat Biotechnol* 2008;26:443–452
- Murtaugh LC. Pancreas and beta-cell development: from the actual to the possible. *Development* 2007;134:427–438
- Jørgensen MC, Ahnfelt-Rønne J, Hald J, Madsen OD, Serup P, Hecksher-Sørensen J. An illustrated review of early pancreas development in the mouse. *Endocr Rev* 2007;28:685–705
- Gittes GK. Developmental biology of the pancreas: a comprehensive review. *Dev Biol* 2009;326:4–35
- Pan FC, Wright C. Pancreas organogenesis: from bud to plexus to gland. *Dev Dyn* 2011;240:530–565
- Kim SK, Hebrok M, Melton DA. Notochord to endoderm signaling is required for pancreas development. *Development* 1997;124:4243–4252
- Hebrok M, Kim SK, Melton DA. Notochord repression of endodermal Sonic hedgehog permits pancreas development. *Genes Dev* 1998;12:1705–1713
- Lammert E, Cleaver O, Melton D. Induction of pancreatic differentiation by signals from blood vessels. *Science* 2001;294:564–567
- Cleaver O, Dor Y. Vascular instruction of pancreas development. *Development* 2012;139:2833–2843
- Schaffer AE, Freude KK, Nelson SB, Sander M. Nkx6 transcription factors and Ptf1a function as antagonistic lineage determinants in multipotent pancreatic progenitors. *Dev Cell* 2010;18:1022–1029
- Sussel L, Kalamaras J, Hartigan-O'Connor DJ, et al. Mice lacking the homeodomain transcription factor Nkx2.2 have diabetes due to arrested differentiation of pancreatic beta cells. *Development* 1998;125:2213–2221
- Prado CL, Pugh-Bernard AE, Elghazi L, Sosa-Pineda B, Sussel L. Ghrelin cells replace insulin-producing beta cells in two mouse models of pancreas development. *Proc Natl Acad Sci U S A* 2004;101:2924–2929
- Castaing M, Duvillé B, Quemeneur E, Basmaciogullari A, Scharfmann R. Ex vivo analysis of acinar and endocrine cell development in the human embryonic pancreas. *Dev Dyn* 2005;234:339–345
- Piper Hanley K, Hearn T, Berry A, et al. In vitro expression of NGN3 identifies RAB3B as the predominant Ras-associated GTP-binding protein 3 family member in human islets. *J Endocrinol* 2010;207:151–161
- Lyttle BM, Li J, Krishnamurthy M, et al. Transcription factor expression in the developing human fetal endocrine pancreas. *Diabetologia* 2008;51:1169–1180
- Polak M, Bouchareb-Banaei L, Scharfmann R, Czernichow P. Early pattern of differentiation in the human pancreas. *Diabetes* 2000;49:225–232
- Piper K, Brickwood S, Turnpenny LW, et al. Beta cell differentiation during early human pancreas development. *J Endocrinol* 2004;181:11–23
- Sarkar SA, Kobberup S, Wong R, et al. Global gene expression profiling and histochemical analysis of the developing human fetal pancreas. *Diabetologia* 2008;51:285–297
- Sugiyama T, Rodriguez RT, McLean GW, Kim SK. Conserved markers of fetal pancreatic epithelium permit prospective isolation of islet progenitor cells by FACS. *Proc Natl Acad Sci U S A* 2007;104:175–180
- Jeon J, Correa-Medina M, Ricordi C, Edlund H, Diez JA. Endocrine cell clustering during human pancreas development. *J Histochem Cytochem* 2009;57:811–824
- Piper K, Ball SG, Keeling JW, Mansoor S, Wilson DI, Hanley NA. Novel SOX9 expression during human pancreas development correlates to abnormalities in Campomelic dysplasia. *Mech Dev* 2002;116:223–226
- Carrasco M, Delgado I, Soria B, Martín F, Rojas A. GATA4 and GATA6 control mouse pancreas organogenesis. *J Clin Invest* 2012;122:3504–3515
- Xuan S, Borok MJ, Decker KJ, et al. Pancreas-specific deletion of mouse Gata4 and Gata6 causes pancreatic agenesis. *J Clin Invest* 2012;122:3516–3528
- Lango Allen H, Flanagan SE, Shaw-Smith C, et al.; International Pancreatic Agenesis Consortium. GATA6 haploinsufficiency causes pancreatic agenesis in humans. *Nat Genet* 2012;44:20–22
- Cleveland MH, Sawyer JM, Afelik S, Jensen J, Leach SD. Exocrine ontogenies: on the development of pancreatic acinar, ductal and centroacinar cells. *Semin Cell Dev Biol* 2012;23:711–719
- Solar M, Cardalda C, Houbracken I, et al. Pancreatic exocrine duct cells give rise to insulin-producing beta cells during embryogenesis but not after birth. *Dev Cell* 2009;17:849–860
- Zhou Q, Law AC, Rajagopal J, Anderson WJ, Gray PA, Melton DA. A multipotent progenitor domain guides pancreatic organogenesis. *Dev Cell* 2007;13:103–114
- Ketola I, Otonkoski T, Pulkkinen MA, et al. Transcription factor GATA-6 is expressed in the endocrine and GATA-4 in the exocrine pancreas. *Mol Cell Endocrinol* 2004;226:51–57
- Decker K, Goldman DC, Grasch CL, Sussel L. Gata6 is an important regulator of mouse pancreas development. *Dev Biol* 2006;298:415–429
- Seymour PA, Freude KK, Tran MN, et al. SOX9 is required for maintenance of the pancreatic progenitor cell pool. *Proc Natl Acad Sci U S A* 2007;104:1865–1870
- Villasenor A, Chong DC, Cleaver O. Biphasic Ngn3 expression in the developing pancreas. *Dev Dyn* 2008;237:3270–3279
- Ostrer H, Wilson DI, Hanley NA. Human embryo and early fetus research. *Clin Genet* 2006;70:98–107
- Miralles F, Czernichow P, Ozaki K, Itoh N, Scharfmann R. Signaling through fibroblast growth factor receptor 2b plays a key role in the

- development of the exocrine pancreas. *Proc Natl Acad Sci U S A* 1999;96:6267–6272
37. Kuo CT, Morrisey EE, Anandappa R, et al. GATA4 transcription factor is required for ventral morphogenesis and heart tube formation. *Genes Dev* 1997;11:1048–1060
  38. Molkenin JD, Lin Q, Duncan SA, Olson EN. Requirement of the transcription factor GATA4 for heart tube formation and ventral morphogenesis. *Genes Dev* 1997;11:1061–1072
  39. Kanai-Azuma M, Kanai Y, Gad JM, et al. Depletion of definitive gut endoderm in Sox17-null mutant mice. *Development* 2002;129:2367–2379
  40. Spence JR, Lange AW, Lin SC, et al. Sox17 regulates organ lineage segregation of ventral foregut progenitor cells. *Dev Cell* 2009;17:62–74
  41. Rodríguez-Seguí S, Akerman I, Ferrer J. GATA believe it: new essential regulators of pancreas development. *J Clin Invest* 2012;122:3469–3471
  42. Pedersen JK, Nelson SB, Jorgensen MC, et al.; Beta Cell Biology Consortium. Endodermal expression of Nkx6 genes depends differentially on Pdx1. *Dev Biol* 2005;288:487–501
  43. Watt AJ, Zhao R, Li J, Duncan SA. Development of the mammalian liver and ventral pancreas is dependent on GATA4. *BMC Dev Biol* 2007;7:37